In Situ Study of Low-Temperature Irradiation-Induced Defects in Silicon Carbide

S.M Tunhuma*, F.D Auret, H.T Danga, J.M Nel, M.M Diale

Department of Physics, University of Pretoria, Private Bag X20, Pretoria 0002, South Africa

Abstract

Ni/4*H*-SiC Schottky barrier diodes have been irradiated by 5.4-MeV helium ions at cryogenic temperatures and their electrical characteristics investigated. Only the prominent native defects ($E_{0.11}$, $E_{0.16}$, and $E_{0.65}$) were observed before and after low-temperature irradiation at 50 K, with a baseline on the spectrum observed starting at 190 K. Low-temperature irradiation reduced the concentration of native $E_{0.11}$ and $E_{0.16}$ defects. After annealing at 380 K, $E_{0.37}$, $E_{0.58}$, $E_{0.62}$, $E_{0.73}$, and $E_{0.92}$ defects were observed. These results show that $E_{0.62}$, an acceptor level of the Z_1 center, and $E_{0.73}$, an acceptor level of the Z_2 center, are both secondary defects which are not formed directly from the irradiation process but from succeeding thermal reactions. An interpretation of the formation of the secondary defects is given.

Keywords: Low-temperature irradiation, DLTS, 4H-SiC, native defects

*corresponding author: S.M Tunhuma email: malven.tunhuma@up.ac.za +27844314906

Introduction

Defects in silicon carbide have become very important for the future. Spin carrying defects have been shown to have great potential for quantum computation applications [1]. These defects are introduced by low temperature irradiation of silicon carbide wafers. In the procedure, irradiation at low temperatures is suggested as a measure to curb contamination and to avoid quasi-reactions of induced defects [2].

Thermodynamically, irradiation induced defects are classified as non-equilibrium defects. They increase the free energy of the material causing it to be more unstable. Gibbs potential is given by [3]

$$\Delta G = \Delta H - T\Delta S \tag{1}$$

where ΔH is the change in enthalpy and ΔS is the entropy When irradiation induced defects are introduced, the increase in enthalpy dominates the increase in entropy [4]. In the presence of sufficient thermal energy the system will try to minimize these defects for stabilization. Low temperature irradiation enables the capture of primary defect species and allows one to study their behaviour as the system stabilizes due to several stimuli [5]. This is important in studying the dynamics and evolution of secondary defects which are observed at higher temperatures when a system has sufficient energy to form them and can shed insights on their nature and occurrence.

Irradiation produces highly mobile point defects and it increases their mobilities. There is formation of quasi-molecules consisting of host and impurity defects after vacancies or interstitials are trapped when mobile. The quasi-molecules which are stable at a particular radiation temperature determine the dominant radiation effects in the semiconductor.

Previous studies on low temperature irradiation induced defects were carried out mainly in germanium and silicon [6-9]. The formation of secondary defects was explained using quasi-chemical reactions of the primary vacancies and interstitials [10]. In n-type silicon, the same set of defects were observed after low temperature irradiation and after room temperature irradiation, whereas in germanium the observed defect sets differed respectively [5].

In silicon carbide, a low temperature irradiation study was carried out using electron paramagnetic resonance (EPR) by Son et.al [11]. They observed various EPR spectra. However the study was not done in-situ but involved transferring samples for measurement.

In this study Ni\4*H*-SiC Schottky barrier diodes were irradiated using He^{2+} ions. The samples were kept at the same temperature in the same set up during irradiation and were not moved at any point during the deep level transient spectroscopy (DLTS) measurements. The results show that at low temperatures only the native defects are detected, all irradiation induced defects reported in the past room temperature studies are a result of succeeding thermal reactions. We describe the possible quasi-reactions that result in the formation of these defects.

Experimental methods and binary collision approximations

The investigated samples were nitrogen doped, n-type,4*H*-silicon carbide epitaxial layers, chemical vapour deposition (CVD) grown on SiC substrates with an ultra-low micropipe density. The net dopant density of the 18 µm thick epi-layers as specified by the suppliers, CREE Inc, was 4.83 × 10^{14} cm^{-3} whilst that of the substrate was ~1 × 10^{18} cm^{-3}. 625 mm^2 samples were degreased for 5 min each in boiling trichloroethylene, acetone and methanol and then etched in hydrofluoric acid. An ohmic contact was formed on the highly doped side by depositing 1000 Åof nickel and annealing at 950 °C for 10 min in argon.

Circular Ni Schottky contacts, 500 Å thick and 0.3 mm in radius were deposited on the epilayer in a resistive evaporator after repeating the cleaning procedure at room temperature. Low temperature irradiation was done in the semiconductor lab at the University of Pretoria using a 5.4 MeV americium-241 radionuclide to a dose of 2.56× 10^{10} cm^{-2}. The irradiation was carried out under a vacuum of ~10^3 mbar in a closed cycle helium cryostat at a temperature of 50 K. Temperature was controlled by a lakeshore 330 temperature controller which heated a sapphire stage on which the sample was placed.

The americium radionuclide is in the form of a foil that can be manually manipulated to come on top of the sample to produce an incident non-monochromatic flux at a 5 mm distance. This is achieved by mounting at the top of the cryostat shroud. A vacuum of ~ 10^{-3} mbar was maintained. DLTS scans were carried out in the 50-380 K range and the data was used to produce log (e_n/T^2) versus 1000/T plots Arrhenius` plots according to the Equation [12]

$$e_n = \sigma_n \langle v_{th} \rangle \frac{g_o}{g_1} N_c \exp\left(-\frac{E_c - E_t}{k_B T} \right) \quad (2)$$

Which gives the emission rate e_n as a function of temperature T the temperature, where v_{th} is the thermal velocity of electrons, (E_c – E_t) is the activation energy, N_c is the density of

conduction band states, g_0 and g_1 are the degeneracy terms of the states before and after electron emission, k_B is the Boltzmann constant and σ_n, the apparent capture cross section.

During DLTS measurements, ionization and external injection of thermalized electrons only alters the charge redistribution on the defects present. As a result the properties of all the defect species were not expected to change because of the scans.

Binary collision approximations were carried out using stopping and range of ions in matter (SRIM) code to estimate the electronic stopping (Se) and ionic stopping (Sn) of the He ions as they migrate into the device. Figure 1 shows the results. The electronic stopping was maximum at the surface and the electronic stopping peaked around 60 µm.

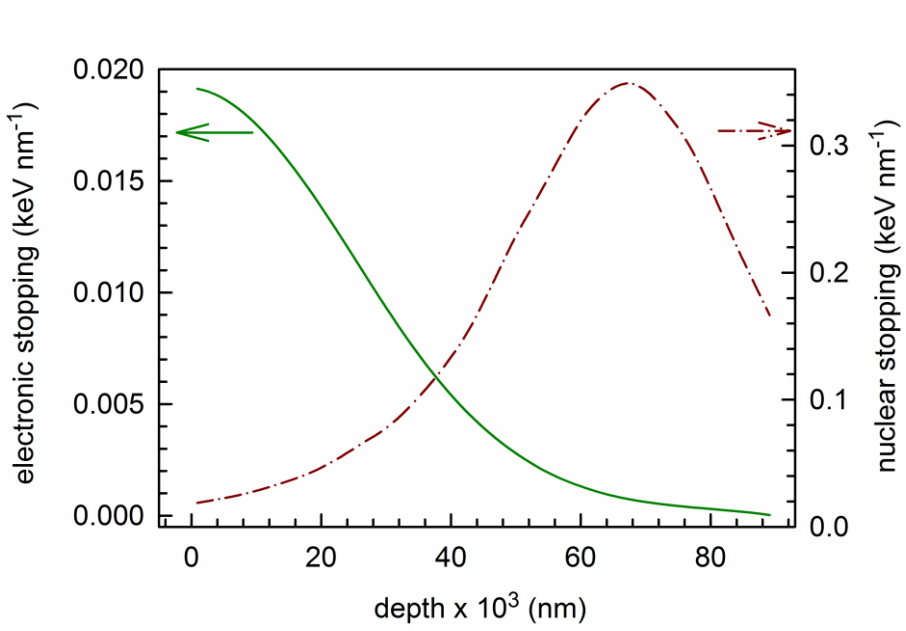

Figure 1: Predicted electronic and nuclear energy with depth obtained from SRIM simulations for 5.4 MeV helium ions on the Ni/4*H*-SiC interface.

Results

Figure 2 shows the DLTS scans obtained at a rate window of 80 Hz. Curve (a) was obtained from the as-deposited samples before irradiation and is for control purposes. It shows the native $E_{0.11}$, $E_{0.16}$ and the $E_{0.65}$ defects whose signatures have been deduced from the Arrhenius` plots in Figure 3. In the nomenclature used $E_{0.11}$ represents a defect level at energy 0.11 eV below the conduction band minima. These native defects have also been reported in CVD grown wafers by other researchers [13]. The $E_{0.11}$ and $E_{0.16}$ have been attributed to titanium impurities [14]. Titanium originates from parts of CVD reactors made from graphite, in which the material is grown or from pumping oil [15]. The $E_{0.65}$ has been identified as the donor level of the Z_2 center [16]

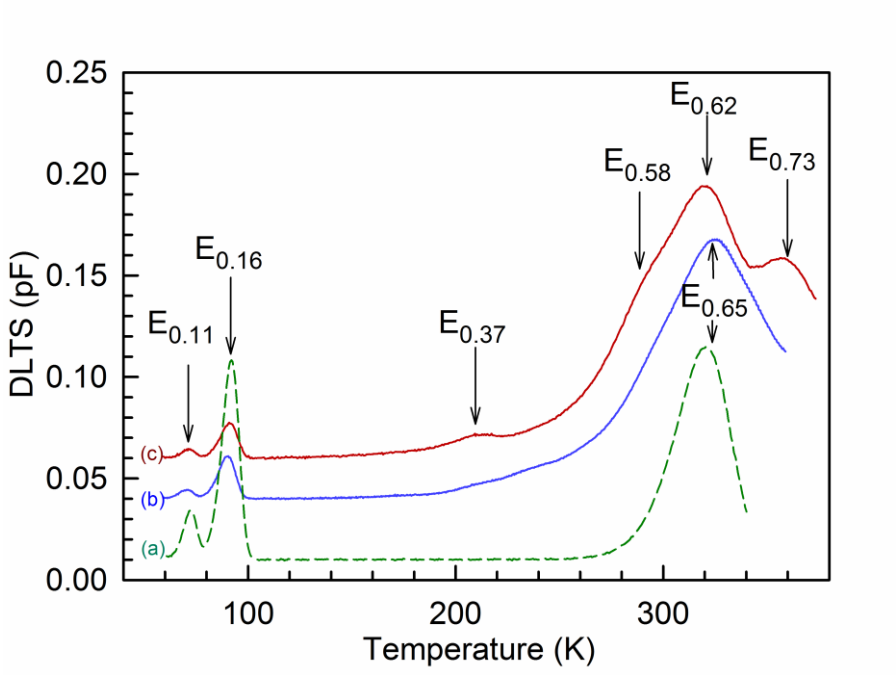

Figure 2 DLTS spectra of (a) The reference spectrum obtained from as-deposited Ni/4*H*-SiC Schottky barrier diodes (b) DLTS spectrum of Ni/4*H*-SiC Schottky barrier diodes irradiated at 50 K (c) DLTS spectrum of Ni/4*H*-SiC Schottky barrier diodes irradiated at 50 K and annealed at 380 K, recorded at a quiescent reverse bias of −5.0 V, rate window of 8 Hz, and a filling pulse of 1 V with a width of 1 ms.

Curve (b) is the scan after low temperature irradiation. It contains the same set of emission peaks as those on curve (a). Incident irradiation forms various defects in semiconductors. As

it slows down in the lattice structure, an implanted ion causes a cascade of inelastic and elastic displacements from collisions with target atoms [17]. The knock on atoms excite or ionize electrons in their passage [18]. The displaced atom may leave a vacancy and occupy a substitutional or interstitial position or vacancy. The introduced defects can be impurities or structural defects, depending on the incident ion mass and differential cross section, total dose, target species and temperature [19]. The defect formation efficiency (σ_D) is given by [20]

$$\sigma_D = \int \frac{\partial^2 \sigma(E,n;E',n')}{\partial E' \partial n'} f(E,n) W(E'n') dn dn' dE dE' \quad (3)$$

Where E is the energy of the incident particle and $E`$ is the energy it transfers to a crystal atom and $n$ is the direction of the incident particle along the crystal axis and $n`$ is the direction after the collision. $f(E,n)$ is the energy distribution function. $W(E`, n`)$ gives the probability that an atom with energy $E`$ and a momentum directed along $n`$ in the collision forms a separate Frenkel pair.

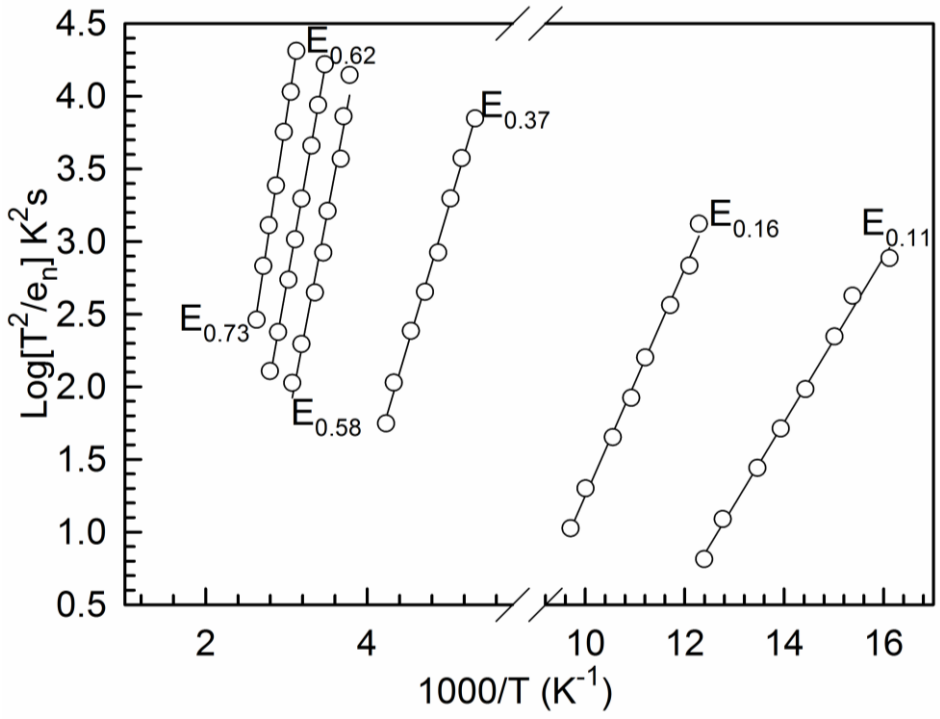

Figure 3 Arrhenius plots of defects introduced in Ni/4*H*-SiC Schottky barrier diodes irradiated at 50 K and annealed at 380 K, recorded at a quiescent reverse bias of −5.0 V, rate window of 8 Hz, and a filling pulse of 1 V with a width of 1 ms.

In this study, helium ions were used, therefore there was a possibility of formation of not only point defects but clusters due to the large size of incident particles. Spatial distribution of vacancy and interstitials is dependent on the defect formation mechanism [21]. If the distance between a vacancy and an interstitial is infinitesimal then they are classified as a Frenkel pair. Frenkel pairs can be formed even at sub-threshold energies which are less than the minimal requirement to initiate a cascade of displacements [18]. Defects generally diffuse to regions of lower concentrations [22]. Upon formation an interstitial moves through the crystal structure and if it encounters a vacancy they combine to form a Frenkel pair or in some cases they recover the solid. At high radiation doses the defects agglomerate to become complexes [23] .

Table 1: Electronic properties of defects introduced in Ni/4*H*-SiC Schottky barrier diodes irradiated at 50 K and annealed at 380 K, recorded at a quiescent reverse bias of −5.0 V, rate window of 8 Hz, and a filling pulse of 1 V with a width of 1 ms.

Defect label	Energy (meV)	σ_n (cm^{-2})
$E_{0.73}$	727	3.9×10^{-15}
$E_{0.62}$	623	1.5×10^{-15}
$E_{0.58}$	583	3.6×10^{-15}
$E_{0.37}$	371	3.8×10^{-16}
$E_{0.16}$	155	1.1×10^{-15}
$E_{0.11}$	113	4.4×10^{-16}

The absence of new defect species on curve (b) after low temperature irradiation suggests that the diffusion of original defects is quenched. However there is a marked decrease in defect concentrations of the $E_{0.11}$ and the $E_{0.16}$. This is accompanied by the introduction of a skewed baseline between 200 and 280 K. The baseline might be introduced as a result of kinetic reactions of the $E_{0.11}$ and the $E_{0.16}$ with the incident irradiation particles as suggested by the correlation between the reductions in defect concentration of the two defects peaks with the introduction of the baseline.

On the same curve (b) a broadening of the $E_{0.65}$ is also observed. Defect diffusion causes a number of reactions including vacancy-interstitial annihilation, vacancy trapping by impurity atoms, and indirect recombination of vacancies and interstitials. There is also a probability of defect arrangement chain reactions.

Curve (c) is the scan after annealing the sample in the cryostat at 380 K. It shows the $E_{0.37}$, $E_{0.58}$, $E_{0.62}$ and the $E_{0.73}$. A result similar to curve (c) was observed by Omotoso et.al after irradiating low doped silicon carbide with 5.4 MeV alpha particles at room temperature [13]. The similarities in their result with ours, suggests that the $E_{0.37}$, $E_{0.58}$, $E_{0.62}$ and the $E_{0.73}$ are secondary defects. The conclusion drawn by Watkins that same defects are produced whether its room temperature or low temperature irradiation in silicon does not hold in silicon carbide [24]. Table 1 lists all the electronic properties of defects observed in this study.

With an increase in sample temperature after irradiation the system comes out of the stability range of some of the defects and further rearrangement of the later may occur. There is interstitial or vacancy hoping into equivalent neighboring positions in the lattice occurring in the course of electron-hole trapping and activation energy-less radiation stimulated diffusion. Ionization radiation also induces defects with repeated alternate capture of holes and electrons termed recombination stimulated diffusion [25]. This migration leads to annihilation reactions of free vacancies and interstitials or formation of quasi-molecules from point defects [26].

Efficiencies of these processes can be described by the cross-section, σ_{AB} of the interaction between any two defects A and B, or by the probability of an elementary reaction between them [27]. This reaction between A and B is obviously affected by their proximity in

distance. Furthermore, these reactions can be accompanied by defect capture by other defects and formation of composite defects from isolated vacancies. Efficiency of Frenkel pair stabilization as opposed to annihilation or vice versa is influenced by the number of impurities present in the lattice structure.

Temperature increase leads to ionization of electrically active defect levels causing the formation of host lattice defects. Under such conditions, carrier concentration rises much more slowly with increasing temperature rather than for self-compensation. The two different processes of defect thermal formation involving no current-carriers followed by independent trapping of a carrier are each characterized by separate and unique activation energies. Self-compensation is when the impurities occupying donor and acceptor sites compensate each other [28]. It may be due to a thermally activated hop of an atom from a lattice site into an interstice, stimulated by a free carrier, trapped at the level of the defect, thus created during its formation.

The $E_{0.58}$, $E_{0.62}$, $E_{0.73}$ can be seen to emanate from the $E_{0.65}$ after alpha particle irradiation. Asghar et al also observed a similar result after irradiating highly doped SiC [29]. They attributed it to the transformation of the Z_1 into the Z_1/Z_2 involving silicon and carbon vacancies as a result of the irradiation. Spatial distribution also influences further reactions during thermal treatment, i.e the possibility of annihilation. Quasi-molecule formation is obviously dependent on the probability of an encounter with an impurity or "defective" atom and the energy barrier to be surmounted in the capture.

The $E_{0.37}$, $E_{0.58}$, $E_{0.62}$, $E_{0.73}$ are within a range that can associate them with the Z_1 and Z_2 centers. According to Eberlein et al, the Z_1 /Z_2 are two negative U centers namely the Z_1 with

a donor level at approximately E_c - 0.43 eV and an acceptor level at approximately E_c - 0.67 eV whilst the Z_2 center has a donor level at E_c – 0.46 eV and an acceptor level at E_c - 0.71 eV [12]. It is evident from Figure 2 (a), (b) and (c) that the defects that are observed after annealing at 380 K are a result of thermodynamic reactions that take place after irradiation according to equation (1).

Son et al combined EPR with DLTS and linked the defects to a carbon vacancy [30]. Trinh et al related it to the acceptor states of the carbon vacancy [31]. Pintile et.al used CVD applying various nitrogen concentrations and suggested that it was a nitrogen complex with carbon interstitials or silicon vacancies [32]. Asghar et.al also linked both defects to silicon vacancies and carbon vacancies after observing them from alpha particle irradiation [29]. It is clear that most if not all models that have been put forward on the identity of the Z_1 and Z_2 are clear on the nature of the defects as vacancies with a negative U behavior. They differ mainly on whether they are carbon or silicon vacancies.

From our results we can speculate that the formation of the negative U centers after irradiation occurs when there is sufficient energy to surpass energy barrier to cause these vacancies to form. It is clear that the Z_1 and Z_2 are secondary defects. They are emanating from thermally assisted diffusion of the primary defects formed by the low temperature irradiation. This occurs as the Gibbs potential of the system is countering the increase in activation enthalpy as a result of the irradiation. The metastable configurations may be due to the adhesion of the vacancies to impurities forming quasi-molecules.

The similarity between the defects observed after low temperature irradiation to those reported by Omotoso et.al show that it is unnecessary to do low temperature irradiations in

the generation of single photon sources. As the resulting defects will be the same after annealing despite the temperature at which they are induced.

Conclusion

Ni/4*H*-SiC Schottky barrier diodes were fabricated using resistive evaporation. The devices were irradiated with He^{2+} ions at 50 K. DLTS scans were carried out in the 50 - 380 K temperature range. Only the native $E_{0.11}$, $E_{0.16}$ and the $E_{0.65}$ defects were observed. After annealing at 380 K, the $E_{0.37}$, $E_{0.58}$, $E_{0.62}$ and the $E_{0.73}$ defects were observed. These defects were attributed to thermally assisted diffusion of primary defects in the lattice structure which agglomerated to form composite defects. The defects observed after annealing are similar to those observed after room temperature irradiation. Unlike in n-type silicon electrically active primary and secondary defects have different identities in 4*H*-SiC. We inferred that low temperature irradiation is not necessary in the generation of single photon sources as post-annealing will result in the same defects despite the temperature at which they are induced

Acknowledgements

The research in this article was funded by the national research foundation (NRF) and the University of Pretoria. The views in this article solely belong to the authors and the NRF accepts no liability. We would like to acknowledge the technical assistance from Dr Mahjoub Ismail.

Bibliography

1. G. V. Astakhov and V. Dyakonov, in Defects in Advanced Electronic Materials and Novel Low Dimensional Structures, ed. Jan Stehr, Buyanova Irina and Chen Weimin (Woodhead Publishing: 2018), pp 211-240.
2. S. Castelletto, B.C. Johnson, V. Ivády, N. Stavrias, T. Umeda, A. Gali and T. Ohshima, Nat. Mater., 13,151, (2014).
3. A. Paul and S. Divinski: Handbook of Solid State Diffusion: Volume 1: Diffusion Fundamentals and Techniques. (Elsevier Science, 2017).
4. B. Cheng and M. Ceriotti, Phys. Rev. B. 97, 054102(2018).
5. A. Mesli, L. Dobaczewski, K. Bonde Nielsen, V. Kolkovsky, M. Christian Petersen and A. Nylandsted Larsen, Phys. Rev. B. 78,165202. (2008).
6. S. Lazanu, I. Lazanu, A. Lepadatu and I. Stavarache, in Semiconductor Conference, 2009. CAS 2009. International, (IEEE: 2009), pp 379-382.
7. P. Nubile, J.C. Bourgoin, D. Stievenard, D. Deresmes and G. Strobl, J. .Appl. Phys. 72, 2673, (1992).
8. L. Khirunenko, M. Sosnin, A. Duvanskii, N.V. Abrosimov and H. Riemann, Solid. State. Phenom. 242, 285,(2015).
9. S. Mäkinen, H. Rajainmäki and Søren Linderoth, Phys. Rev. B. (Condens Matter Mater Physics) 42, 11166,1990
10. L. I. Khirunenko, V. I. Shakhovtsov and V. V. Shumov, Semiconductors. 32, 120, (1998).
11. N.T. Son, J. Isoya, N. Morishita, T. Ohshima, H. Itoh, A. Gali and E. Janzén, Mater. Scie. Forum, 377,(2009).
12. D.K. Schroder: Semiconductor Material and Device Characterization. (Wiley, 2006).
13. A. T. Paradzah, F. D. Auret, M. J. Legodi, E. Omotoso and M. Diale, Nucl. Instrum. Methods Phys. Res., Sect. B. 358, 112, (2015)
14. S. M. Tunhuma, F. D. Auret, M. J. Legodi, J. Nel and M. Diale, Mater. Scie. Semicond. Process. 81,122, (2018).
15. T. Dalibor, G. Pensl, N. Nordell and A. Schöner, Phys. Rev. B. 55, 13618,(1997).
16. T. A. G. Eberlein, R. Jones and P. R. Briddon, Phys. Rev. Lett.90, 225502,(2003).
17. M.S. Dresselhaus and R. Kalish: Ion Implantation in Diamond, Graphite and Related Materials. (Springer Berlin Heidelberg, 2013).
18. C. Leroy: Principles of Radiation Interaction in Matter and Detection (4th Edition). (World Scientific Publishing Company Pte Limited, 2015).
19. J. D. Haskell, W. A. Grant, G. A. Stephens and J. L. Whitton, In Ion Implantation in Semiconductors, ed. Ingolf Ruge and Graul Jürgen (Springer Berlin Heidelberg: 1971), pp 193-198.
20. V. L. Vinetskii and G. A. Kholodar, in Modern Problems in Condensed Matter Sciences, ed. R. A. Johnson and Orlov A. N. (Elsevier: 1986), pp 283-344.
21. C. Claeys and E. Simoen: Radiation effects in advanced semiconductor materials and devices. (Springer Science & Business Media, 2013).
22. R. Hou, L. Li, X. Fang, Z. Xie, S. Li, W. Song, R. Huang, J. Zhang, Z. Huang, Q. Li, W Xu, Engang Fu and G. G. Qin, Nucl. Instrum. Methods Phys. Res., Sect. B. 414, 74, (2018).
23. E. Rimini: Ion Implantation: Basics to Device Fabrication. (Springer US, 2013).
24. F.L. Vook and S. Laboratory: Radiation Effects in Semiconductors: Proceedings. (Plenum Press, 1968).
25. P. Pichler: Intrinsic Point Defects, Impurities, and Their Diffusion in Silicon. (Springer Vienna, 2004).
26. A.M. Stoneham: Theory of Defects in Solids: Electronic Structure of Defects in Insulators and Semiconductors. (Clarendon Press, 2001).
27. W. Wesch and E. Wendler: Ion Beam Modification of Solids: Ion-Solid Interaction and Radiation Damage. (Springer International Publishing, 2016).
28. W. Walukiewicz, In Wide-gap chalcopyrites, (Springer: 2006), pp 35-54.
29. M. Asghar, I. Hussain, H. S. Noor, F. Iqbal, Q. Wahab and A. S. Bhatti, J. Appl. Phys.101, 073706, (2007).
30. N. T Son, X. Thang Trinh, L.S. Løvlie, B.G. Svensson, K. Kawahara, J. Suda, T. Kimoto, T. Umeda, J. Isoya and T. Makino, Phys. Rev. lett. 109, 187603, (2012).
31. X. T. Trinh, K. Szász, T. Hornos, K. Kawahara, J. Suda, T. Kimoto, A. Gali, E. Janzén and N. T. Son, Phys. Rev. B. 88, 235209, (2013).
32. I. Pintilie, L. Pintilie, K. Irmscher and B. Thomas, Appl. Phys. Lett. 81, 4841, 2002.